

**Isolation and characterization of novel polymorphic microsatellite loci for the deep-sea hydrothermal vent limpet, *Lepetodrilus nux*, and the vent-associated squat lobster, *Shinkaia crosnieri***

Yuichi Nakajima, Chuya Shinzato, Mariia Khalturina, Masako Nakamura, Hiromi Kayama Watanabe, Satoshi Nakagawa, Noriyuki Satoh, Satoshi Mitarai

Y. Nakajima (corresponding author), S. Mitarai

Marine Biophysics Unit, Okinawa Institute of Science and Technology Graduate University, Onna, Okinawa 904-0495, Japan

Tel: +81 98 966 1669; Fax: +81 98 966 1064

e-mail: [yuichi.nakajima@oist.jp](mailto:yuichi.nakajima@oist.jp); [yuichi.nakajima@outlook.com](mailto:yuichi.nakajima@outlook.com)

C. Shinzato

Atmosphere and Ocean Research Institute, The University of Tokyo, Kashiwa, Chiba 277-8564, Japan

M. Khalturina, N. Satoh

Marine Genomics Unit, Okinawa Institute of Science and Technology Graduate University, Onna, Okinawa 904-0495, Japan

M. Nakamura

School of Marine Science and Technology, Tokai University, Shimizu, Shizuoka 424-8610, Japan

H. K. Watanabe

Japan Agency for Marine-Earth Science and Technology, Yokosuka, Kanagawa 237-0061, Japan

S. Nakagawa

Division of Applied Biosciences, Graduate School of Agriculture, Kyoto University, Kitashirakawa,  
Kyoto 606-8502, Japan

### **Abstract**

Recent genetic research has begun to reveal population structures of deep-sea, hydrothermal vent species, but detailed assessments of genetic diversity and connectivity in hydrothermal vent populations, based on multiple genetic loci are still scarce, especially in the Northwest Pacific. Accordingly, we isolated 38 novel polymorphic microsatellite loci from the limpet, *Lepetodrilus nux*, and 14 from the squat lobster, *Shinkaia crosnieri*, two dominant hydrothermal vent species, using next-generation sequencing. These loci revealed polymorphism levels of 5–20 alleles per locus in *L. nux* and 5–25 in *S. crosnieri*. Observed and expected heterozygosities ranged from 0.240 to 0.960 and 0.283 to 0.938 in *L. nux* and from 0.450 to 0.950 and 0.620 to 0.941 in *S. crosnieri*, respectively. Twelve loci in *L. nux* and four loci in *S. crosnieri* showed significant deviation from Hardy-Weinberg equilibrium ( $p < 0.05$ ). Microsatellite loci evaluated in this study will enable detailed measurements of genetic diversity and connectivity among populations, and better understanding of evolutionary divergence processes of *L. nux* and *S. crosnieri* in deep-sea communities in the Northwest Pacific.

**Keywords:** Chemosynthetic ecosystem, Northwest Pacific, nuclear genetic marker, Okinawa Trough,

population genetics, simple sequence repeat

## **Introduction**

Various invertebrate species occur in deep-sea, chemosynthetic ecosystems such as hydrothermal vents and cold seeps (reviewed in Van Dover et al. 2002; Vrijenhoek 2010). Larval dispersal is critical for population maintenance and colonization via migration in deep-sea environments (e.g., Adams et al. 2012). Most vent invertebrates have free-swimming larval phases that drift with ocean currents (see Vrijenhoek 2010). To quantify divergence and connectivity of deep-sea populations, recent genetic research has investigated the population structure of hydrothermal vent-endemic gastropods and vent-associated decapods, using polymorphic nuclear microsatellite loci (e.g., Southwest Pacific: Thaler et al. 2011, 2014; Scotia Sea: Roterman et al. 2016). Given that more deep-sea environments will be exploited for mining (Vrijenhoek 2010), conservation genetics research will require more profound understanding of genetic diversity and connectivity based on multiple genetic loci. Detailed assessments of genetic diversity and connectivity based on individual genetic identification are still scarce due to the paucity of genetic markers, especially in deep-sea populations of the Northwest Pacific, which is one of the most likely deep-sea mining targets (Nakajima et al. 2015).

To provide genetic tools for the estimation of genetic connectivity, we isolated and characterized novel polymorphic microsatellite loci of the lepetodrilid limpet, *Lepetodrilus nux*, and the galatheid squat lobster, *Shinkaia crosnieri*, using next-generation sequencing. These species are the most abundant invertebrates in the Okinawa Trough, and they often co-exist, with many *L. nux* attached to the exoskeleton of *S. crosnieri* (Fig. 1A, B). With the development of next-generation sequencing technology, recent studies focusing on single nucleotide polymorphism (SNP) (reviewed in Davey et al. 2011)

revealed genetic differentiation and immigration patterns for some deep-sea species (*Bathymodiolus*, Breusing et al. 2016; Xu et al. 2016). Genome-level studies require high-quality genome sequencing to obtain proper polymorphism data and a large number of *de novo* SNP loci in the absence of reference genomes. Genome-wide SNP analysis may not be applicable for preserved samples; therefore, microsatellites are necessary for high-quality genetic data when using previously collected samples.

The genus *Lepetodrilus* (Family Lepetodrilidae) is the most abundant and diverse gastropod group at deep-sea hydrothermal vents (Desbruyères et al. 2006), and some *Lepetodrilus* species colonize cold seeps, wood falls, and whale carcasses (Johnson et al. 2008). Previous studies have reported molecular phylogenetic and evolutionary relationships among species or populations in the genus *Lepetodrilus* using allozymes or mitochondrial genes (Vrijenhoek et al. 1997; Johnson et al. 2006, 2008; Matabos et al. 2008; Plouviez et al. 2009; Nakamura et al. 2014). Roterman et al. (2013) isolated and characterized microsatellite loci of an undescribed species of *Lepetodrilus* at the East Scotia Ridge in the South Atlantic Ocean. Using these microsatellites, Roterman et al. (2016) reported that *Lepetodrilus* sp. in the Southern Ocean did not show genetic differentiation of populations separated by as much as 440 km. Populations on the ridge were significantly differentiated from populations on a caldera only ~95 km apart, but there was a difference of ~1,000 m in depth between the ridge and caldera. However, no microsatellite loci from other *Lepetodrilus* species have been reported. *Lepetodrilus nux* is widely distributed and abundant at hydrothermal vents in the Okinawa Trough (Okutani et al. 1993; Sasaki et al. 2003; Nakamura et al. 2014). This species has not been found in other regions. In contrast, the genus *Shinkaia* (Family Munidopsidae) has only a single species, *S. crosnieri*. This species has been found at the Edison Seamount in the Bismarck Archipelago, Okinawa Trough, and near northeastern Taiwan (Baba and Williams 1998; Chan et al. 2000). It was recently found near southwestern Taiwan and inhabits both

hydrothermal vents and cold methane seeps (Yang et al. 2016). Microsatellite loci from *S. crosnieri* have not been previously reported. Microsatellite loci developed in this study will be useful in population genetic studies to estimate genetic diversity, assess genetic connectivity among populations, and better understand pelagic larval migration patterns and evolutionary processes of deep-sea hydrothermal vent invertebrates in the Northwest Pacific.

## Methods

Genomic DNA of *L. nux* and *S. crosnieri* (one individual each) for sequencing was isolated using proteinase K with phenol-chloroform extraction. Extracted genomic DNA was purified using ethanol precipitation and a QIAquick PCR purification kit (Qiagen). DNA samples were fragmented into approximately 200-300-bp lengths using the DNA Shearing System M220 (Covaris inc.), and genomic libraries with approximately 300-bp insert lengths were prepared using a TruSeq DNA LT Sample Prep Kit – Set A (Illumina). DNA sequencing employed 300-bp, paired-end reads, using a MiSeq sequencer (Illumina) with a MiSeq Reagent Kit v3, 600 cycles (Illumina), according to manufacturer's instructions. Illumina sequencing adapters were trimmed with fastq-mcf in ea-utils ver. 1.1.2-537 (Aronesty 2011) and sequences of overlapping read pairs were assembled using fastq-join in ea-utils. Assembled sequences longer than 100-bp were selected. Simple sequence repeats (SSRs) were detected and polymerase chain reaction (PCR) primers were designed for each assembled sequence using PAL\_FINDER ver. 0.02.04 (Castoe et al. 2012). Next, we removed redundancies in the assembled sequences using CDHIT-EST (Li and Godzik 2006). We selected primer pairs amplifying repeat stretches for isolation of highly variable loci with these thresholds: 10 repeats or more for 3 to 6 mer SSRs for *L. nux*; 10 repeats or more for 3 and 4 mer SSRs for *S. crosnieri*.

For characterization of microsatellite loci, we screened 25 individuals of *L. nux* and 40 individuals of *S. crosnieri*, collected near hydrothermal vents in the Iheya North field of the Okinawa Trough (27°47.412' N/126°54.037' E, at 1,058 m depth for *L. nux* and 27°47.455' N/126°53.796' E, at 979 m depth for *S. crosnieri*) (Fig. 1C). Collection was accomplished during a cruise of the Research Vessel 'Natsushima' (Cruise No. NT13-22 for *L. nux* and No. NT07-13 for *S. crosnieri*), using the remotely operated vehicle (ROV) 'Hyper-Dolphin' (Dive No. HPD#1592 for *L. nux* and HPD#711 for *S. crosnieri*). Specimens were preserved in 99.5% ethanol and then transferred to the laboratory. Genomic DNA was extracted using a DNeasy Tissue Extraction Kit (Qiagen). We performed PCR to amplify and to estimate polymorphism at selected microsatellite loci. The PCR reaction mixture (5 µL) contained <100 ng of template genomic DNA, AmpliTaq Gold 360 Master Mix (Thermo Fisher Scientific), and three primers for each locus: a non-tailed forward primer (final concentration 0.5 µM in the mixture), a reverse primer with a U19 (5' -GGTTTTCCCAGTCACGACG-3) tail (final 0.5 µM), and a U19 primer (final 0.5 µM) fluorescently labeled with FAM, VIC, NED, or PET (see Schuelke 2000). PCR was performed with denaturation at 94°C for 5 min, followed by 35 cycles of denaturation at 95°C for 30 s, annealing at 56°C for 30 s, extension at 72°C for 1 min, and a final extension at 72°C for 5 min. Fragment analysis for determination of PCR product length was subsequently conducted with the capillary-based DNA sequencer ABI 3130xl Genetic Analyzer (Thermo Fisher Scientific) and GeneMapper ver. 3.7 (Thermo Fisher Scientific).

For successfully amplified microsatellite loci showing one or two distinct allelic peak(s) in the fragment analysis, the number of alleles, expected and observed heterozygosity, and  $F_{IS}$  as a deviation index from the Hardy-Weinberg equilibrium (HWE) were calculated using GenAlEx ver. 6.501 (Peakall and Smouse 2006). Micro-Checker ver. 2.2.3 (Van Oosterhout et al. 2004) was utilized to detect the effect

of null alleles for each locus at 95% and 99% confidence levels by performing 10,000 randomizations. Null allele frequency, assuming HWE, was assessed with the Van Oosterhout null allele estimator (see instructions for Micro-Checker). For all successfully amplified loci, linkage disequilibrium was estimated using Genepop (<http://genepop.curtin.edu.au/>) (Raymond and Rousset 1995; Rousset 2008) under the following Markov chain parameters: 1,000 dememorizations, 100 batches, 1,000 iterations per batch. Significance level was adjusted using a false discovery rate (FDR) correction (Benjamini and Hochberg 1995).

## **Results and Discussion**

For *L. nux*, we obtained 305,155,974 bp (803,122 read pairs) of raw sequence data from genomic DNA, and each read pair was assembled. We used the 764,173 assembled sequences longer than 100 bp (147,673,155 bp, average 193 bp) for SSR identification with PAL\_FINDER. Ninety-six primer pairs were selected for designing microsatellite primer pairs (3 mer repeats: 69 loci, 4 mer: 22, 5 mer: 3, 6 mer: 2). From these 96 pairs, 38 loci were successfully amplified and characterized (Table 1). Three of these 38 (L<sub>nux\_10</sub>, L<sub>nux\_67</sub>, and L<sub>nux\_68</sub>) showed non-amplification in one or two individuals. The number of alleles per locus ranged from five to 20, and the values of observed and expected heterozygosities ranged from 0.240 to 0.960 and 0.283 to 0.938, respectively. Twelve loci showed significant deviation from HWE ( $p < 0.05$ ). Nine and three of these 12 loci indicated deficits and excesses, respectively, of observed heterozygosity. Analysis with Micro-Checker identified 11 loci with possible null alleles. If these 11 loci show null alleles in other populations as well, they will not be suitable for population genetic study. Nonetheless, it is possible that loci lacking null alleles in our samples still may not be useful for other populations due to genotyping errors. Significant linkage disequilibrium after FDR

correction was detected in the combination of L<sub>nux\_20</sub> and L<sub>nux\_42</sub> ( $p < 0.001$ ).

For *S. crosnieri*, we obtained 559,780,016 bp (1,603,392 read pairs) and each read pair was assembled as described above. We used the 15,256 assembled sequences longer than 100 bp (3,377,044 bp, average 221 bp). Ninety-six primer pairs were selected to design microsatellite primer pairs (3 mer repeats: 48 loci, 4 mer: 48). Using these 96 pairs, 14 loci were successfully amplified and characterized (Table 2). One of the 14 loci (Scro\_27) failed to amplify in one individual. The number of alleles per locus ranged from 5 to 25, and the values of observed and expected heterozygosities ranged from 0.450 to 0.950 and 0.620 to 0.941, respectively. Four loci showed significant deviation from HWE ( $p < 0.05$ ), and all of these indicated deficits of observed heterozygosity. Analysis with Micro-Checker identified eight loci with possible null alleles. No significant linkage disequilibrium after FDR correction was detected (all  $p > 0.05$ ).

The novel polymorphic microsatellite markers isolated and characterized in this study will be available for population genetics of *L. nux* and *S. crosnieri*. Genetic identification of individuals using microsatellites may facilitate development of more detailed connectivity patterns of these invertebrates among sites. Based on studies of the mitochondrial COI gene, it is known that populations of *L. nux* maintain a high degree of genetic diversity and connectivity among four vent fields in the Okinawa Trough that are separated by approximately 550 km, (Nakamura et al. 2014). Larvae of *Lepetodrilus* and *S. crosnieri* are lecithotrophic (Lutz et al. 1984; Miyake et al. 2010; Vrijenhoek 2010). Further analysis using multiple genetic markers may show moderate or high gene flow with evidence of stochastic stepping-stone dispersal among sites (Vrijenhoek 1997; Vrijenhoek 2010). With genetic connectivity data, recent physical modeling by Mitarai et al. (2016) will also be helpful for estimation of larval migration patterns among vents at ecological time scales. In addition, Yang et al. (2016) identified intraspecific

genetic differentiation of *S. crosnieri* between vents and cold methane seeps using the mitochondrial COI gene; however, there was no significant differentiation in the adenine nucleotide translocase gene. Future investigations will be expected to detail the genetic differentiation among sites. Microsatellites will permit detailed genetic diversity and connectivity estimates among populations separated geographically and occurring at different depths. Such studies will reveal evolutionary divergence processes in these deep-sea communities in the Northwest Pacific.

### **Acknowledgments**

We are grateful to Dr. Hiroyuki Yamamoto, chief scientist of the KR12-02 and NT13-22 cruises, and to officers and crews of the 'Natsushima,' and the operation team of ROV 'Hyper-Dolphin' for collecting the specimens. This work was financially supported by The Canon Foundation and Okinawa Institute of Science and Technology Graduate University. We thank Dr. Steven D. Aird (Okinawa Institute of Science and Technology Graduate University) for editing the manuscript.

### **References**

Adams DK, Arellano SM, Govenar B (2012) Larval dispersal: vent life in the water column. *Oceanography* 25:256–268

Aronesty E (2011) ea-utils: "Command-line tools for processing biological sequencing data". <http://code.google.com/p/ea-utils>

Baba K, Williams AB (1998) New Galatheoidea (Crustacea, Decapoda, Anomura) from hydrothermal

systems in the West Pacific Ocean: Bismarck Archipelago and Okinawa Trough. *Zoosystema* 20:143–156

Benjamini Y, Hochberg Y (1995) Controlling the false discovery rate: a practical and powerful approach to multiple testing. *J Roy Statist Soc B* 57:289–300

Breusing C, Biastoch A, Drews A, Metaxas A, Jollivet D, Vrijenhoek RC, Bayer T, Melzner F, Sayavedra L, Petersen JM, Dubilier N, Schilhabel MB, Rosenstiel P, Reusch TBH (2016) Biophysical and population genetic models predict the presence of "phantom" stepping stones connecting Mid-Atlantic Ridge vent ecosystems. *Curr Biol* 26:2257–2267

Castoe TA, Poole AW, De Koning AP, Jones KL, Tomback DF, Oyler-McCance SJ, Fike JA, Lance SL, Streicher JW, Smith EN, Pollock DD (2012) Rapid microsatellite identification from Illumina paired-end genomic sequencing in two birds and a snake. *PLoS One* 7:e30953

Chan TY, Lee DA, Lee CS (2000) The first deep-sea hydrothermal animal reported from Taiwan: *Shinkaia crosnieri* Baba and Williams, 1998 (Crustacea: Decapoda: Galatheidae). *Bull Mar Sci* 67:799–804

Davey JW, Hohenlohe PA, Etter PD, Boone JQ, Catchen JM, Blaxter ML (2011) Genome-wide genetic marker discovery and genotyping using next-generation sequencing. *Nat Rev Genet* 12:499–510

Desbruyères D, Segonzac M, Bright M (2006) Handbook of Deep-sea Hydrothermal Vent Fauna. Denisia

18, Linz, Austria

Johnson SB, Young CR, Jones WJ, Warén A, Vrijenhoek RC (2006) Migration, isolation, and speciation of hydrothermal vent limpets (Gastropoda; Lepetodrilidae) across the Blanco Transform Fault. *Biol Bull* 210:140–157

Johnson SB, Warén A, Vrijenhoek RC (2008) DNA barcoding of *Lepetodrilus* limpets reveals cryptic species. *J Shellfish Res* 27:43–51

Li W, Godzik A (2006) Cd-hit: a fast program for clustering and comparing large sets of protein or nucleotide sequences. *Bioinformatics* 22:1658–1659

Lutz RA, Jablonski D, Turner RD (1984) Larval development and dispersal at deep-sea hydrothermal vents. *Science* 226:1451–1454

Matabos M, Thiébaud E, Le Guen D, Sadosky F, Jollivet D, Bonhomme F (2008) Geographic clines and stepping-stone patterns detected along the East Pacific Rise in the vetigastropod *Lepetodrilus elevatus* reflect species crypticism. *Mar Biol* 153:545–563

Mitarai S, Watanabe H, Nakajima Y, Shchepetkin AF, McWilliams JC (2016) Quantifying dispersal from hydrothermal vent fields in the western Pacific Ocean. *Proc Nat Acad Sci USA* 113:2976–2981

Miyake H, Kitada M, Itoh T, Nemoto S, Okuyama Y, Watanabe H, Tsuchida S, Inoue K, Kado R, Ikeda S, Nakamura K, Omata T (2010) Larvae of deep-sea chemosynthetic ecosystem animals in captivity. *Cah Biol Mar* 51:441–451

Nakajima R, Yamamoto H, Kawagucci S, Takaya Y, Nozaki T, Chen C, Fujikura K, Miwa T, Takai K (2015) Post-drilling changes in seabed landscape and megabenthos in a deep-sea hydrothermal system, the Iheya North Field, Okinawa Trough. *PLoS One* 10:e0123095

Nakamura M, Watanabe H, Sasaki T, Ishibashi J, Fujikura K, Mitarai S (2014) Life history traits of *Lepetodrilus nux* in the Okinawa Trough, based upon gametogenesis, shell size, and genetic variability. *Mar Ecol Prog Ser* 505:119–130

Okutani T, Fujikura K, Sasaki T (1993) New taxa and new distribution records of deepsea gastropods collected from or near the chemosynthetic communities in the Japanese waters. *Bull Natl Sci Mus Tokyo A* 19:123–143

Peakall R, Smouse PE (2006) GENALEX 6: genetic analysis in Excel. Population genetic software for teaching and research. *Mol Ecol Notes* 6:288–295

Plouviez S, Shank TM, Faure B, Daguin-Thiebaut C, Viard F, Lallier FH, Jollivet D (2009) Comparative phylogeography among hydrothermal vent species along the East Pacific Rise reveals vicariant processes and population expansion in the South. *Mol Ecol* 18:3903–3917

Raymond M, Rousset F (1995) Genepop (version 1.2): population genetics software for exact tests and ecumenicism. *J Hered* 86:248–249

Roterman CN, Copley JT, Linse KT, Tyler PA, Rogers AD (2013) Development of polymorphic microsatellite loci for three species of vent-endemic megafauna from deep-sea hydrothermal vents in the Scotia Sea, Southern Ocean. *Conserv Genet Resour* 5:835–839

Roterman CN, Copley JT, Linse KT, Tyler PA, Rogers AD (2016) Connectivity in the cold: the comparative population genetics of vent-endemic fauna in the Scotia Sea, Southern Ocean. *Mol Ecol* 25:1073–1088

Rousset F (2008) Genepop'007: a complete reimplementation of the Genepop software for Windows and Linux. *Mol Ecol Resour* 8:103–106

Sasaki T, Okutani T, Fujikura K (2003) New taxa and new records of patelliform gastropods associated with chemoautosynthesis-based communities in Japanese waters. *Veliger* 46:189–210

Schuelke M (2000) An economic method for the fluorescent labeling of PCR fragments. *Nat Biotechnol* 18:233–234

Thaler AD, Zelnio K, Saleu W, Schultz TF, Carlsson J, Cunningham C, Vrijenhoek RC, Van Dover CL

(2011) The spatial scale of genetic subdivision in populations of *Ifremeria nautiliei*, a hydrothermal-vent gastropod from the southwest Pacific. *BMC Evol Biol* 11:372

Thaler AD, Plouviez S, Saleu W, Alei F, Jacobson A, Boyle EA, Schultz TF, Carlsson J, Van Dover CL (2014) Comparative population structure of two deep-sea hydrothermal-vent-associated decapods (*Chorocaris* sp. 2 and *Munidopsis lauensis*) from southwestern Pacific back-arc basins. *PLoS One* 9:e101345

Van Dover CL, German CR, Speer KG, Parson LM, Vrijenhoek RC (2002) Evolution and biogeography of deep-sea vent and seep invertebrates. *Science* 295:1253–1257

Van Oosterhout C, Hutchinson WF, Wills DPM, Shipley P (2004) MICRO-CHECKER: software for identifying and correcting genotyping errors in microsatellite data. *Mol Ecol Notes* 4:535–538

Vrijenhoek RC (1997) Gene flow and genetic diversity in naturally fragmented metapopulations of deep-sea hydrothermal vent animals. *J Hered* 88:285–293

Vrijenhoek RC, Feldman RA, Lutz RA, Craddock C, Hashimoto J (1997) Genetic characterization of *Lepetodrilus* limpets from hydrothermal vents in the Mariana Trough. *JAMSTEC Journal of Deep Sea Research*, Special Volume “Deep sea research in subduction zones, spreading centers and backarc basins”, pp 111–116

Vrijenhoek RC (2010) Genetic diversity and connectivity of deep-sea hydrothermal vent metapopulations.

Mol Ecol 19:4391–4411

Xu T, Sun J, Lv J, Watanabe HK, Li T, Zou W, Rouse GW, Wang S, Qian P-Y, Bao Z, Qiu J-W (2016)

Genome-wide discovery of single nucleotide polymorphisms (SNPs) and single nucleotide variants (SNVs) in deep-sea mussels: Potential use in population genomics and cross-species application. Deep

Sea Res II: doi.org/10.1016/j.dsr2.2016.03.011

Yang C-H, Tsuchida S, Fujikura K, Fujiwara Y, Kawato M, Chan T-Y (2016) Connectivity of the squat

lobsters *Shinkaia crosnieri* (Crustacea: Decapoda: Galatheidae) between cold seep and hydrothermal vent

habitats. Bull Mar Sci 92:17–31

## Figure and Tables

### Figure 1

A. Specimens of *Lepetodrilus nux* attached to the exoskeleton of *Shinkaia crosnieri*. *Lepetodrilus nux* are indicated with red arrow. B. Vent fauna, including *L. nux* and *S. crosnieri*, in the Iheya North field. These individuals comprise a vent faunal community. The deep-sea brown mussel belongs to the genus *Bathymodiulus*, and some of these also have *L. nux* on their shells. The photo was taken during a cruise in the Iheya North field (Cruise No. KR12-02, Dive No. 7K#537). C. Map of the sampling location for *L. nux* and *S. crosnieri*. The Iheya North field is located in the Okinawa Trough, Northwest Pacific region.

### Table 1

Characteristics of 38 polymorphic microsatellite loci from 25 specimens of *Lepetodrilus nux*: locus name, primer sequences, repeat motif, size range including U19 tail, the number of alleles ( $N_A$ ), observed ( $H_o$ ) and expected ( $H_E$ ) heterozygosities, deviation index from HWE ( $F_{is}$ ), null allele frequency (Null freq.), and GenBank accession number.

\* Individuals whose DNA was not successfully amplified (\*1 individual, \*\*2 individuals).

† Significant deviation from HWE († $p < 0.05$ , †† $p < 0.01$ , ††† $p < 0.001$ ).

‡ Possible presence of null alleles, estimated by Micro-Checker (‡ $p < 0.05$ , ‡‡ $p < 0.01$ ).

### Table 2

Characteristics of 14 polymorphic microsatellite loci from 40 specimens of *Shinkaia crosnieri*: locus name, primer sequences, repeat motif, size range including U19 tail, the number of alleles ( $N_A$ ), observed ( $H_o$ ) and expected ( $H_E$ ) heterozygosities, deviation index from HWE ( $F_{is}$ ), null allele frequency (Null freq.), and GenBank accession number.

\* An individual whose DNA was not successfully amplified.

† Significant deviation from HWE († $p < 0.05$ , †† $p < 0.001$ ).

‡ Possible presence of null alleles, estimated by Micro-Checker (‡ $p < 0.05$ , ‡‡ $p < 0.01$ ).

Figure 1

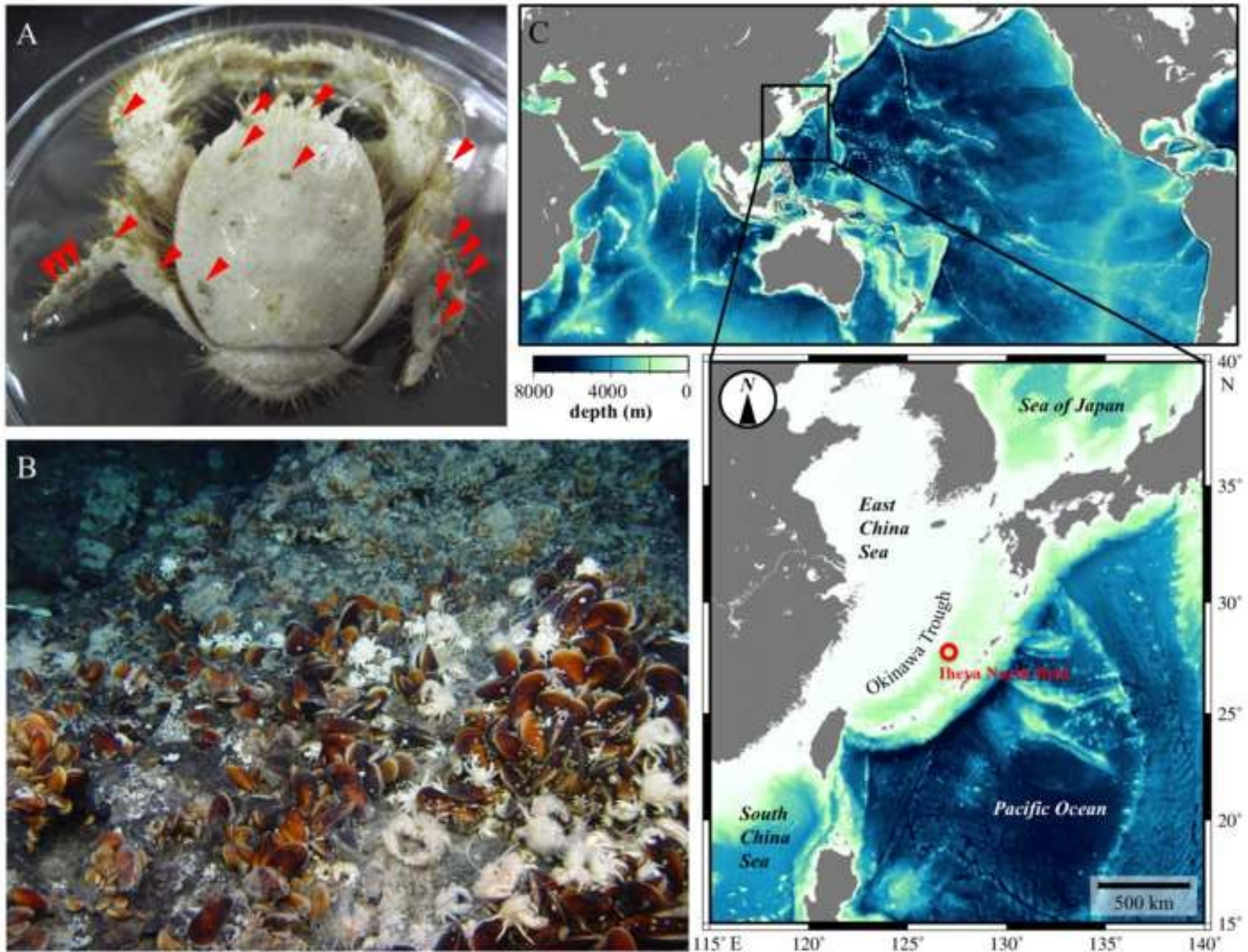


Table 1

Locus	Repeat motif	Forward primer sequence (5'-3')	Reverse primer sequence (5'-3')	Size range (bp)	$N_A$	$H_O$	$H_E$	$F_{IS}$	Null freq.	Accession No.
L <sub>nu</sub> x_10**	(TCAC) <sub>12</sub>	AAGATTCCAGGCTGTGACG	U19-TCACTGCGATGACTCTTTCC	119-209	12	0.565	0.863	0.345 <sup>††</sup>	0.166 <sup>‡‡</sup>	AB971595
L <sub>nu</sub> x_12	(TATG) <sub>13</sub>	U19-TCGGATCGGGGTTGG	GACCTTGAGCTGGGTTCCG	145-211	15	0.880	0.879	-0.001	0.001	AB971596
L <sub>nu</sub> x_16	(TGTCG) <sub>12</sub>	ATCATTATCGGTGAAATTCG	U19-TGCATAGAACGTTTGG	158-193	8	0.800	0.778	-0.029	-0.021	AB971597
L <sub>nu</sub> x_18	(TCAT) <sub>13</sub>	TGGAGAGTCGCTGAACTGG	U19-CCTTTGATACAGAGAACG	155-191	9	0.840	0.762	-0.102	-0.058	AB971598
L <sub>nu</sub> x_20	(CCACAT) <sub>10</sub>	U19-ACAGAGGGGTGATATCCG	CAGAATGACGGAACCTGGC	144-241	14	0.560	0.865	0.352 <sup>†††</sup>	0.178 <sup>‡‡</sup>	AB971599
L <sub>nu</sub> x_22	(TCAA) <sub>10</sub>	U19-AATATTCCTGCTGCGATGC	TGATTCAGCTGACCAGGC	95-134	8	0.400	0.814	0.508 <sup>†††</sup>	0.249 <sup>‡‡</sup>	AB971600
L <sub>nu</sub> x_23	(TATC) <sub>23</sub> (CATC) <sub>4</sub>	TTGAGTTACCATCATCTGGC	U19-TCAACGTACTIONCCATGTGCC	145-254	17	0.960	0.910	-0.055	-0.031	AB971601
L <sub>nu</sub> x_24	(AGTG) <sub>12</sub>	TTGTCGCCACTCTTGTAGG	U19-TGTGTTGGATCGTGTATGGG	106-141	11	0.440	0.858	0.487 <sup>†††</sup>	0.242 <sup>‡‡</sup>	AB971602
L <sub>nu</sub> x_29	(TAA) <sub>14</sub>	TATCCAACCCAAGCTGCC	U19-CCTCGGAGATCAATATGC	179-212	10	0.760	0.747	-0.017 <sup>†</sup>	-0.014	AB971603
L <sub>nu</sub> x_30	(TAC) <sub>15</sub> (AAT) <sub>4</sub>	U19-ACCGTTACACAGGGATGC	CCACGATTTCTTAAAGGC	190-227	12	0.920	0.838	-0.097	-0.050	AB971604
L <sub>nu</sub> x_33	(AGA) <sub>15</sub>	U19-TTGTATTGCCGTGTGACG	ACCTAATCCCCTCCCC	142-220	15	0.760	0.899	0.155	0.078 <sup>‡</sup>	AB971605
L <sub>nu</sub> x_34	(ATA) <sub>15</sub>	TCCAGGATACACAAACAAGC	U19-AGGTCAAAAATGCTCTGCC	144-175	10	0.920	0.824	-0.117 <sup>††</sup>	-0.065	AB971606
L <sub>nu</sub> x_40	(TAG) <sub>15</sub> AAGTAA(TAG) <sub>4</sub>	CATTGATACCGGGCTCC	U19-CCAACGTCTACCACTGCG	133-154	8	0.680	0.799	0.149 <sup>††</sup>	0.078	AB971607
L <sub>nu</sub> x_42	(ATA) <sub>15</sub>	CCCTTGTGAAGGTACTIONTGGC	U19-ACAAGCATGGGAGCATGG	152-196	13	0.840	0.862	0.026	0.017	AB971608
L <sub>nu</sub> x_45	(ATT) <sub>15</sub> (AGT) <sub>13</sub>	U19-AGGAATTATGACCAGGAGG	ATTCAGTTGGAACGTCGC	135-205	20	0.880	0.938	0.061	0.031	AB971609
L <sub>nu</sub> x_46	(AAT) <sub>15</sub> N <sub>12</sub> (AAAT) <sub>3</sub> AACAC C(AAC) <sub>3</sub>	U19-GAAGCATCTCAATTTACCC	AAGCTCGAGCATGTATTTGG	140-185	12	0.640	0.842	0.240	0.122 <sup>‡‡</sup>	AB971610
L <sub>nu</sub> x_54	(TAC) <sub>20</sub> TAT(TAA) <sub>6</sub>	ACCAGTAGTTGATCGCAGG	U19-TGTTCACTIONTCCAACGGG	168-193	9	0.920	0.793	-0.160	-0.087	AB971611
L <sub>nu</sub> x_55	(AGT) <sub>3</sub> AGG(AGT) <sub>20</sub>	TGAAAGCAACTCTAAACCCC	U19-CAAATAATGGCAAGTAAGG	116-200	18	0.720	0.917	0.215 <sup>†††</sup>	0.110 <sup>‡‡</sup>	AB971612
L <sub>nu</sub> x_59	(AGT) <sub>20</sub> AAC(ACT) <sub>3</sub>	ATTTTACATGTACTIONTTCGCGG	U19-TCGACGACAGGTTAATGC	132-205	18	0.800	0.914	0.124	0.061 <sup>‡</sup>	AB971613
L <sub>nu</sub> x_63	(AGT) <sub>20</sub>	TATCTGTACCCCTCTTCGG	U19-AAAGCGACTCTAAACCCC	120-168	17	0.760	0.912	0.167	0.082 <sup>‡‡</sup>	AB971614
L <sub>nu</sub> x_66	(CTA) <sub>20</sub>	U19-AGGATTGGCATGATCC	GGCATATGTGAGCCGGG	108-181	17	0.680	0.899	0.244	0.125 <sup>‡‡</sup>	AB971615
L <sub>nu</sub> x_67*	(ATT) <sub>4</sub> N <sub>9</sub> (AGT) <sub>5</sub> (TAG) <sub>23</sub>	TTTGGAGCATGGAATTGG	U19-TGCGTTAAATGATTCTCG	158-229	20	0.625	0.930	0.328 <sup>††</sup>	0.166 <sup>‡‡</sup>	AB971616
L <sub>nu</sub> x_68*	(GTA) <sub>24</sub>	U19-GAAACCTGCAACATCCG	TGTGATGCGGAACTGTTCG	119-164	10	0.750	0.841	0.108	0.055	AB971617
L <sub>nu</sub> x_69	(CTA) <sub>23</sub>	AATGGCAACATTATTTACAG	U19-ACAAACACATTATTGCGCC	137-223	16	0.880	0.914	0.038	0.017	AB971618
L <sub>nu</sub> x_70	(TGT) <sub>6</sub> TAT(TGT) <sub>4</sub> TAT(TGA) <sub>21</sub>	U19-TCTTATCATGATCGCGTCC	CAATGTCCGGTGAATAAGTGC	161-214	16	0.960	0.915	-0.049	-0.025	AB971619

Lnu <sub>x</sub> _71	(ATC) <sub>20</sub>	TTCTTTGAGTTCAATTTGCC	U19-TGCTTATATTTTGCTGCTCG	137-221	15	0.880	0.873	-0.008	-0.005	AB971620
Lnu <sub>x</sub> _74	(TCA) <sub>10</sub>	AATAATCGTCGTCATCACCG	U19-AACAACAATGCCCCTGG	107-141	10	0.720	0.716	-0.006 <sup>††</sup>	-0.012	AB971621
Lnu <sub>x</sub> _78	(ATA) <sub>10</sub>	U19-CTTTGATGGTGTGAATCG	TCAATGAAGCTCATGAATGC	90-111	7	0.520	0.670	0.223	0.100	AB971622
Lnu <sub>x</sub> _79	(CTT) <sub>3</sub> N <sub>9</sub> (CAT) <sub>3</sub> CAG(CAT) <sub>10</sub>	CCGCGAGTATCATAATGCC	U19-ATGTAGAAATTGCGCCCG	161-213	16	0.880	0.891	0.013	0.003	AB971623
Lnu <sub>x</sub> _81	(ATA) <sub>10</sub>	U19-TTAAGGGTTTTGTTGGCG	AAAGCTCTTTGGAAGTAGCC	152-167	5	0.480	0.557	0.138	0.066	AB971624
Lnu <sub>x</sub> _83	(ATT) <sub>10</sub>	U19-CTGAATGCAGCCCTGG	TCATGAAAAGGGTGTATTGG	180-192	5	0.240	0.283	0.153	0.056	AB971625
Lnu <sub>x</sub> _84	(TCA) <sub>10</sub>	U19-ACCACTGAGCACCTTCGG	CCTGGAGGAGGGACAAGG	138-156	7	0.520	0.510	-0.019	0.011	AB971626
Lnu <sub>x</sub> _88	(CTA) <sub>3</sub> GTACTG(CTA) <sub>10</sub> CTG (CTA) <sub>7</sub> CCT(CTA) <sub>5</sub>	GTGGTGATACTGACGCCG	U19-GCTTTCGTGAATAGAAGG	154-197	13	0.840	0.858	0.021 <sup>†</sup>	0.006	AB971627
Lnu <sub>x</sub> _91	(ATA) <sub>10</sub>	TTTATCGAATGTTGCACAGC	U19-TCTTTGTCTGCGCTTCG	147-171	9	0.680	0.766	0.112	0.056	AB971628
Lnu <sub>x</sub> _92	(AAT) <sub>10</sub>	U19-CCAAAATGACACCAGCACC	TTCCACATGGAGTCCAGC	132-153	8	0.600	0.570	-0.053	-0.067	AB971629
Lnu <sub>x</sub> _94	(TAA) <sub>10</sub>	U19-TTGGTGAAATGTCATGAGG	AGTGGGTGGATATGGCG	120-132	5	0.720	0.550	-0.308	-0.223	AB971630
Lnu <sub>x</sub> _95	(ATT) <sub>10</sub>	U19-GGTGAAATATCCCACTGC	CACGGTAAAACCTGAATGGG	155-195	9	0.840	0.833	-0.009	0.000	AB971631
Lnu <sub>x</sub> _96	(ATG) <sub>10</sub>	ATTCGTTGAAACGTACTIONCG	U19-TATCCTTTCGAGCGTGG	126-162	8	0.720	0.774	0.070 <sup>††</sup>	0.031	AB971632

---

Table 2

Locus	Repeat motif	Forward primer sequence (5'-3')	Reverse primer sequence (5'-3')	Size range (bp)	$N_A$	$H_O$	$H_E$	$F_{IS}$	Null freq.	Accession No.
Scro_06	(CTAT) <sub>20</sub>	AGAACAACCTCGCGTTGC	U19-AGCCACAGCGTTACAGCC	147-248	18	0.700	0.921	0.240	0.121 <sup>**</sup>	LC152883
Scro_12	(AGGT) <sub>22</sub>	CAGGCTGACAGGCAAACG	U19-AAAGGGGACAGGATGG	138-263	23	0.950	0.925	-0.027	-0.015	LC152884
Scro_17	(CTTC) <sub>16</sub>	CCTACCTATTCTCCCTCCG	U19-TGGAGGTGTGAGTGAGGG	168-232	19	0.825	0.918	0.101	0.050 <sup>‡</sup>	LC152885
Scro_27*	(ATCT) <sub>17</sub>	U19-TTCTGTGCATCCATCCC	TGACGAGGGAATTAGGAAGG	207-341	20	0.872	0.922	0.055 <sup>†††</sup>	0.026	LC152886
Scro_40	(TATC) <sub>10</sub>	U19-TCAATTATCCGGCAACGG	TGAAAGCCCATGGTACGG	176-196	5	0.550	0.620	0.113	0.062	LC152887
Scro_43	(GGAA) <sub>10</sub>	U19-ATGAGGGAGGTGAATGG	TGGAAGGTCTAGATTGATCG	85-113	7	0.450	0.673	0.331 <sup>†††</sup>	0.167 <sup>**</sup>	LC152888
Scro_44	(ATAG) <sub>6</sub> ATAA(ATAG) <sub>10</sub>	U19-AAGGCCTTTTGTCTGTGG	GCTAGGTCTGATATGCCTCG	189-249	13	0.600	0.748	0.198 <sup>†††</sup>	0.097 <sup>‡</sup>	LC152889
Scro_45	(GGAA) <sub>10</sub>	U19-TGAGGGGAGGTAGAGAGG	CTCTCATTCTGTCTGTTCC	123-178	11	0.650	0.795	0.182	0.090 <sup>‡</sup>	LC152890
Scro_52	(ACG) <sub>20</sub> N <sub>12</sub> (ACA) <sub>3</sub>	U19-TAACCTGGTGGCTGTCTG	AATATATCGCCCGTCCTGC	184-229	8	0.700	0.670	-0.044	-0.020	LC152891
Scro_56	(TAT) <sub>20</sub>	TGTATTTTCAGCTTTCGGGC	U19-ACAAACGACCCAACACCC	120-182	14	0.800	0.853	0.062 <sup>†</sup>	0.026	LC152892
Scro_57	(TAT) <sub>19</sub> TACAAT(TAT) <sub>19</sub>	GTCGCCGAATCTGTTTCC	U19-CAGTCGGGTCACCTCG	199-301	25	0.775	0.941	0.176	0.087 <sup>**</sup>	LC152893
Scro_66	(AAT) <sub>15</sub>	AACGGGTAAATGTTTGACGC	U19-ACCGCATTTCTTTTCGC	112-263	15	0.550	0.701	0.215	0.104 <sup>**</sup>	LC152894
Scro_88	(AAT) <sub>10</sub>	CCCCAAACCTCCACC	U19-AGCCACAAGATGACG	89-121	11	0.750	0.694	-0.080	-0.057	LC152895
Scro_90	(CTC) <sub>2</sub> CTT(CTC) <sub>3</sub> N <sub>14</sub> (CTC) <sub>3</sub> (CTT) <sub>2</sub> (CTC) <sub>10</sub>	CACTCAATCACTCCTCCTCC	U19-TGGTGCATCGTGAGAGG	150-209	11	0.650	0.786	0.173	0.086 <sup>‡</sup>	LC152896